

Supplementary Information

Autologous extracellular vesicles derived from conjunctival squamous cell carcinoma deliver therapeutic microRNAs to induce apoptosis in originating cancer

Suresh Thangudu, Sourabh Mehta, Hala Shakib Dhowre, Sanja Bojic, Golnaz Haghverdi,
Albert Wu, Tarik F Massoud, and Ramasamy Paulmurugan

Canary Center for Cancer Early Detection, Molecular Imaging Program at Stanford, Bio-X Program, Stanford University School of Medicine, Palo Alto, California 94304, United States

Corresponding author:

Ramasamy Paulmurugan and Tarik F Massoud
Molecular Imaging Program at Stanford (MIPS),
Canary Center for Cancer Early Detection
Department of Radiology
Stanford University School of Medicine
3155 Porter Drive, Room: 2236
Palo Alto, CA 94304
Phone: 650-725-6097 (Office); 650-804-4987 (Cell), Fax: 650-721-6921
E-mail: paulmur8@stanford.edu; tmassoud@stanford.edu

and:

Albert Y. Wu
Department of Ophthalmology
Stanford Byers Eye Institute
Stanford University School of Medicine
Palo Alto, CA 94303, USA
Email: awu1@stanford.edu

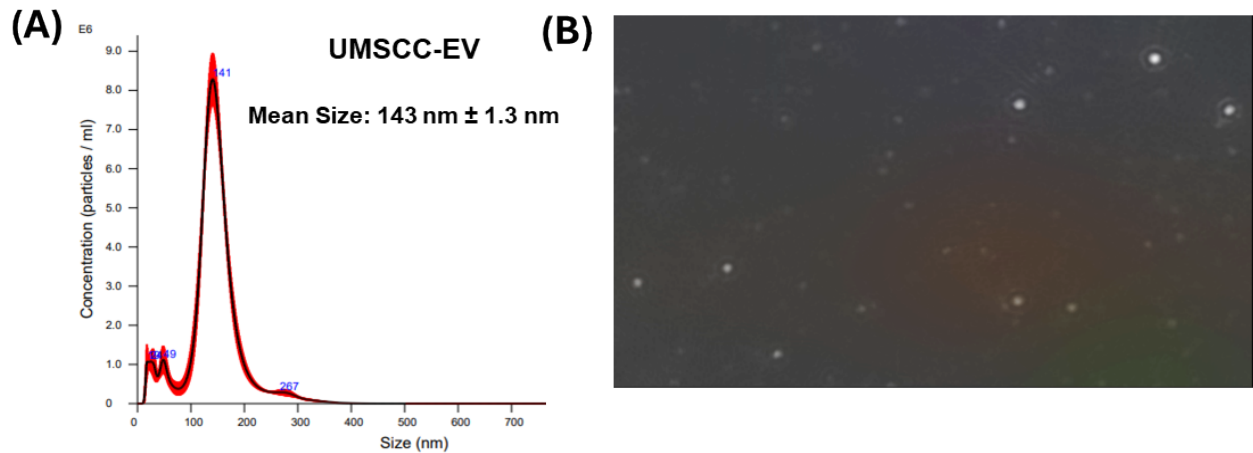


Figure S1. (A) NTA analysis of UMSSC9 cell-derived EVs. (B) NTA microscopy image of EVs.

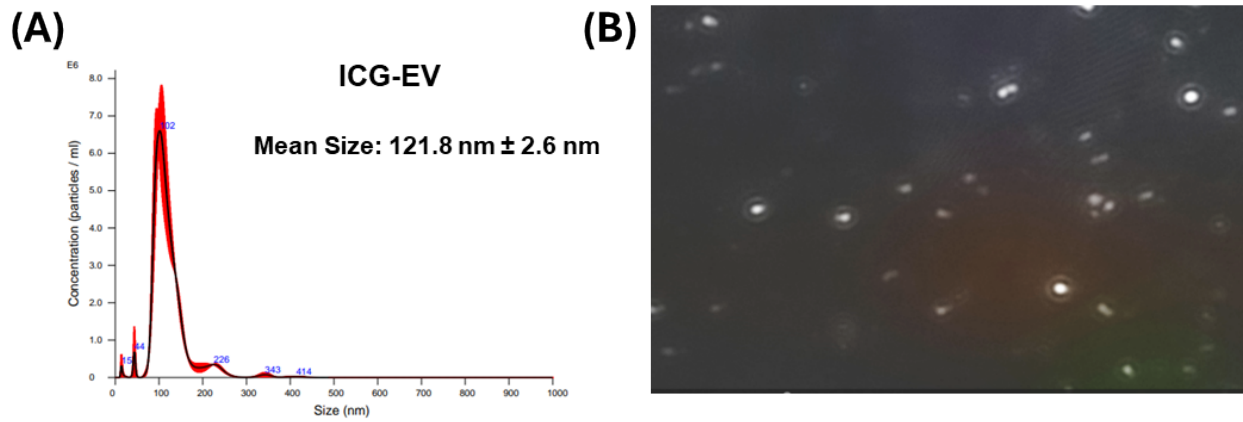


Figure S2. (A) NTA analysis of ICG-conjugated EVs after microfluidics. (B) NTA microscopy image of microfluidic reconstructed EVs.

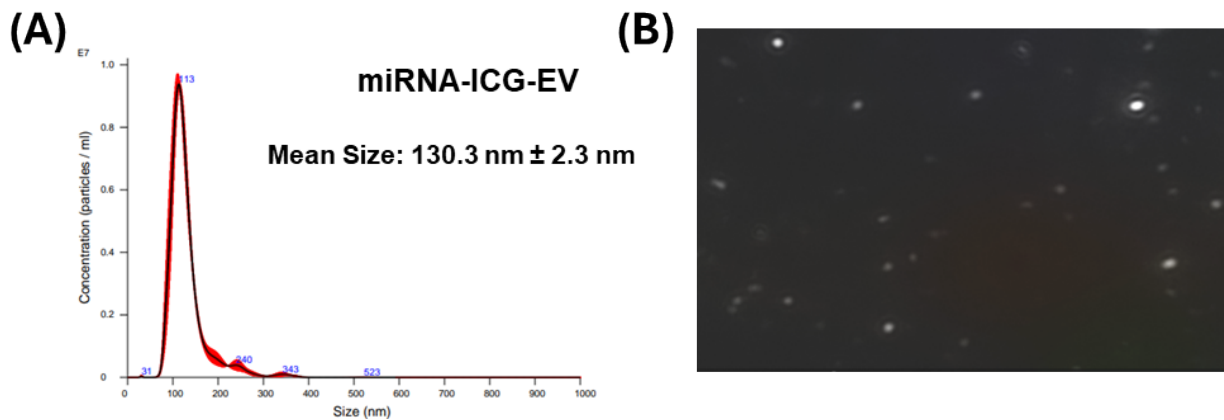


Figure S3. (A) NTA analysis of Cy5-antimiRNA-10b loaded ICG-EVs after microfluidics. (B) NTA microscopy image of microfluidic reconstructed EVs.

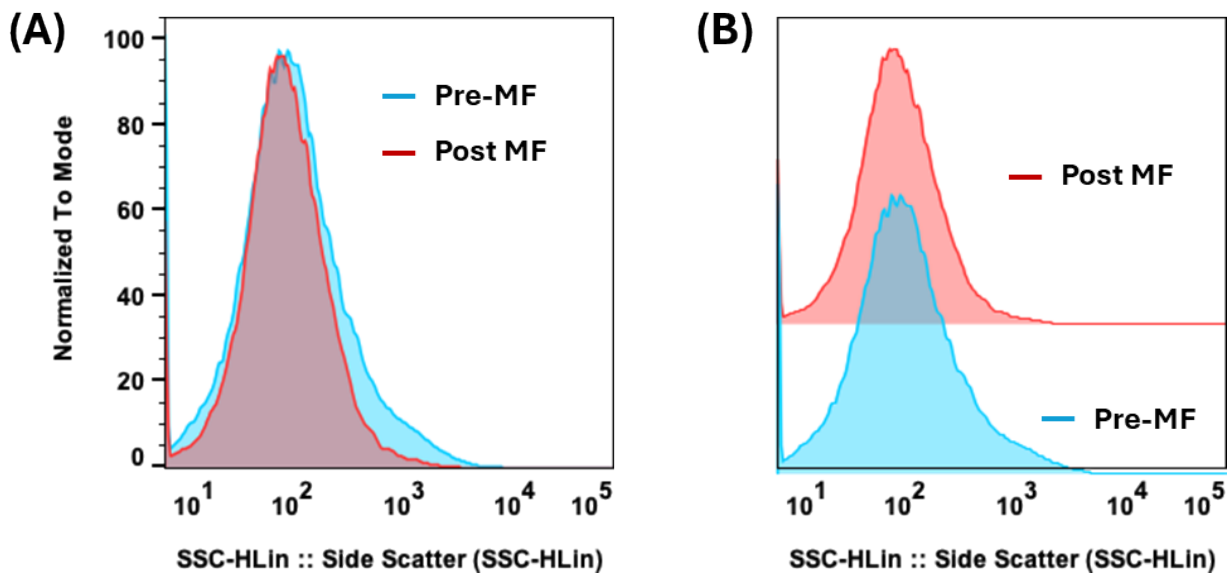


Figure S4. (A) & (B) Overlaid and half-max set FACS plots of EVs before and after microfluidics mediated reconstruction, respectively, analyzed using side scattering window.

Figure S5. ICG-EVs and Cy5-antimiRNA-10b encapsulated ICG-EVs after resolved in SDS-PAGE and imaged using the IVIS optical imaging system. ICG imaging window (left) and Cy5 imaging window (right).

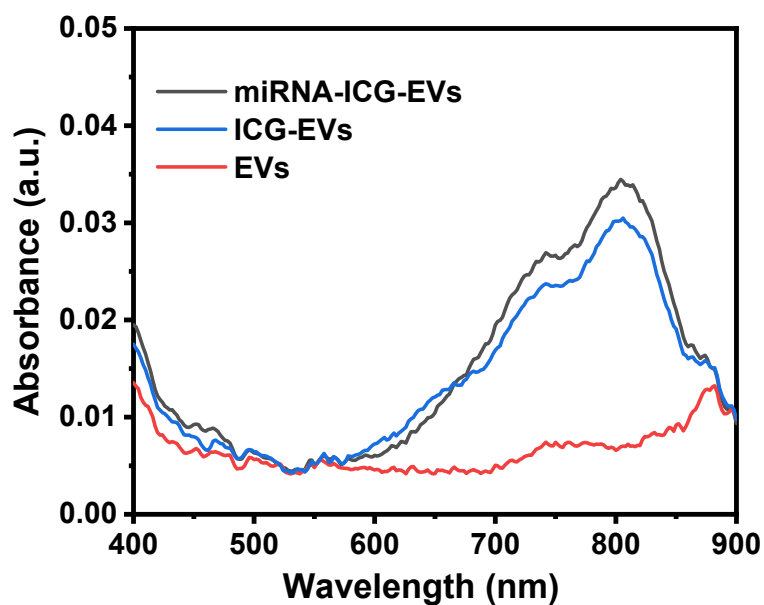


Figure S6. UV-visible absorption spectra of EVs, ICG-EVs and miRNA-ICG-EVs showing the peak in the NIR region. (Experimental condition: each sample was suspended in PBS prior to measurements).

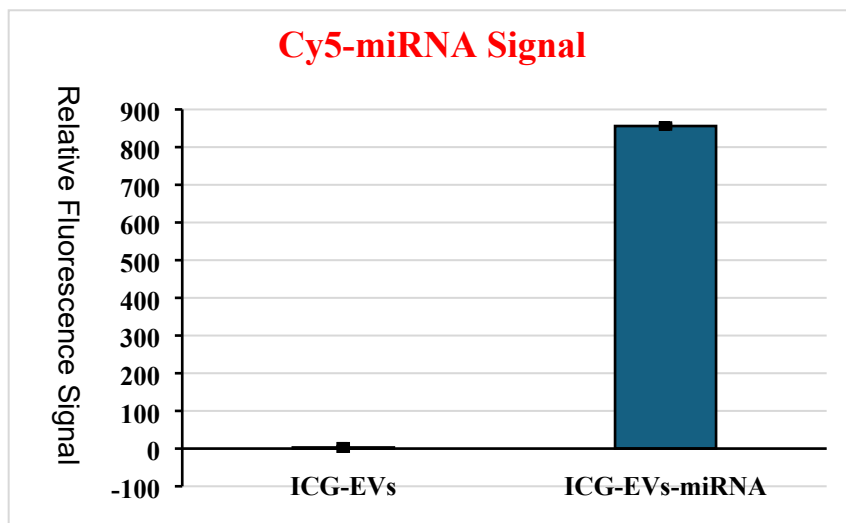


Figure S7. Fluorescent emission intensity signal measured spectroscopically for Cy5-anti-miR-10b loaded ICG-EVs (microRNA Cy5-anti-miRNA-10b-ICG-EVs) in comparison to ICG-EVs under Cy5 excitation wavelength.

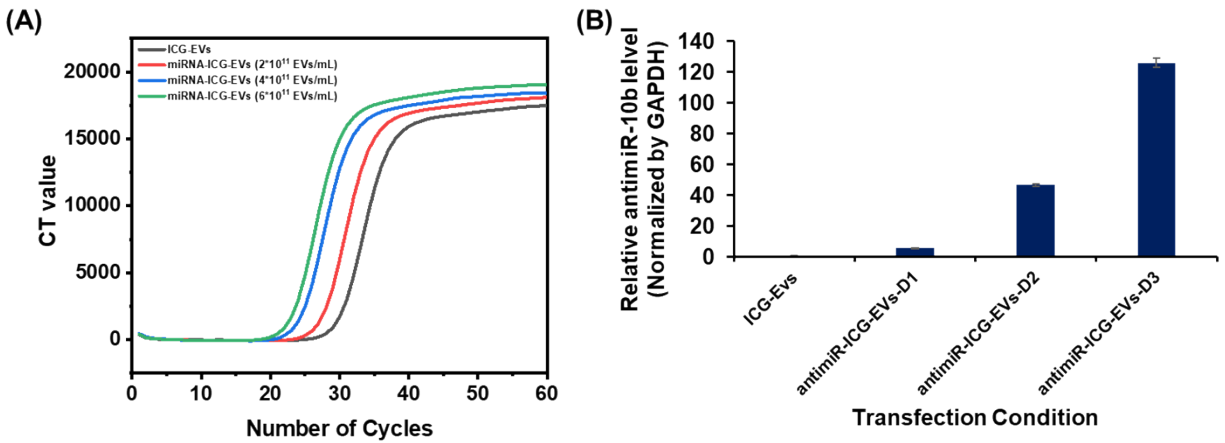


Figure S8. (A) Quantitative graph showing the RT-PCR spectra of anti-miR-10b amplified using the RNA isolated from UMSCC9 cells transfected using miRNA-ICG-EVs formulations in different concentration (2×10¹¹ EVs/mL; 4×10¹¹ EVs/mL; 6×10¹¹ EVs/mL). (B) Relative levels of delivered anti-miRNA-10b after normalized using GAPDH (D1: 2×10¹¹ EVs/mL; D2: 4×10¹¹ EVs/mL; D3: 6×10¹¹ EVs/mL).

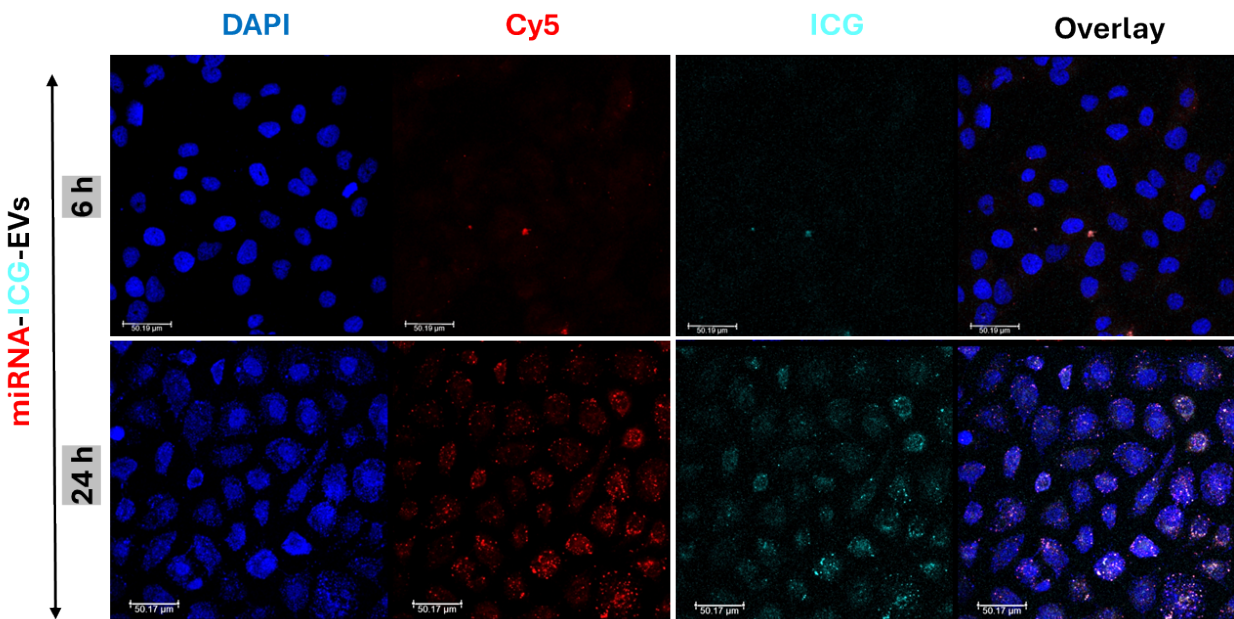


Figure S9. Time dependent cellular internalization of Cy5-miRNA-ICG-EVs into UMSCC9 cancer cells (Cy5-miRNA-ICG-EVs at a concentration of 4 × 10⁹ ; scale bar: 50 μm).

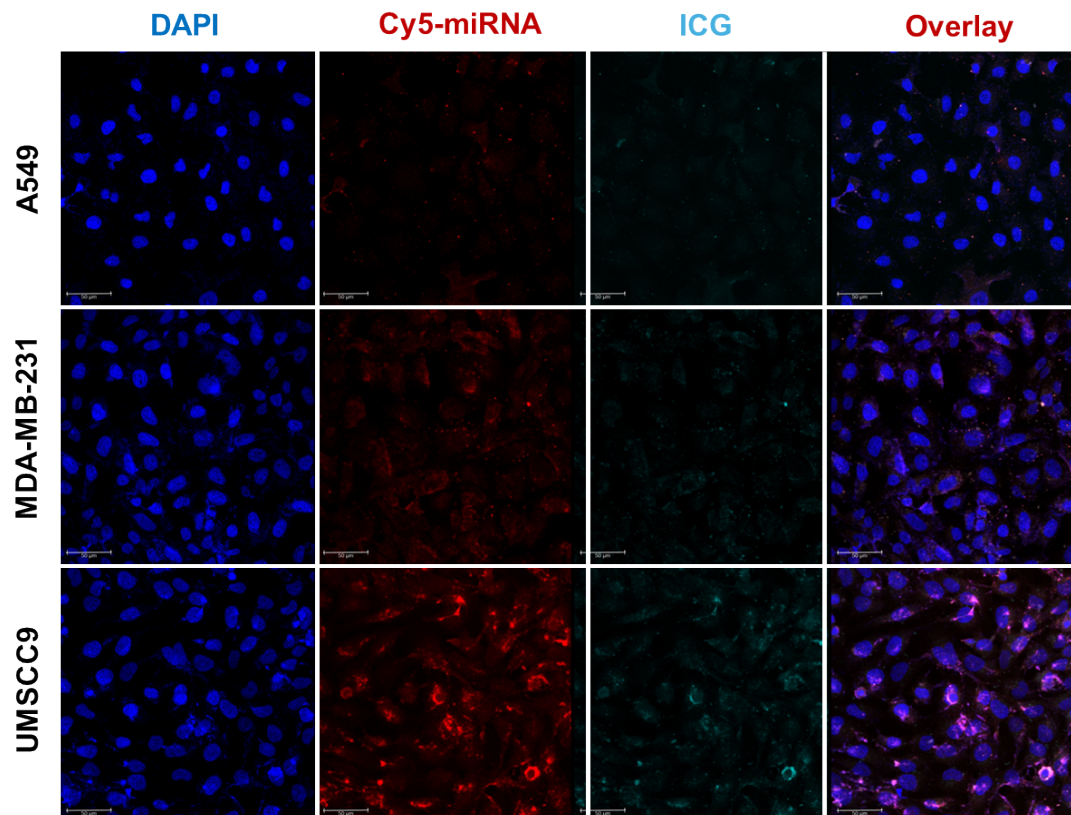


Figure S10. Cellular internalization of Cy5-miRNA-ICG-EVs in A549, MDA-MB-231 and UMSCC9 cells. The cells were treated with Cy5-miRNA-ICG-EVs at a concentration of 12×10^9 for 10 h of incubation time and laser confocal microscopic images were obtained after staining with DAPI; scale bar: 50 μm).

Z stack imaging (each slice thickness is 1 μM)

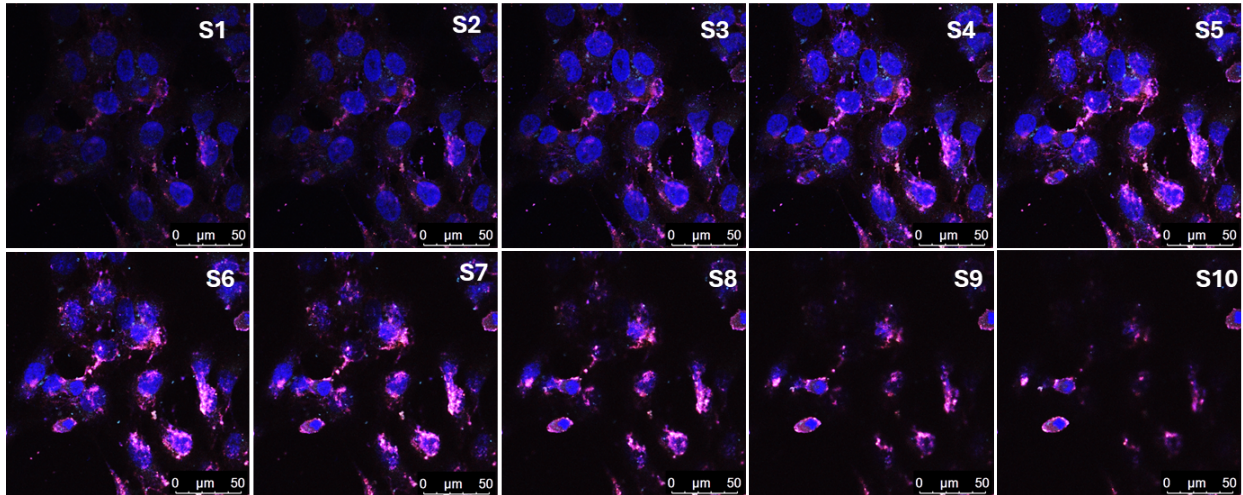
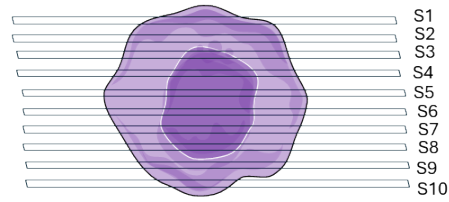


Figure S11. Z-stack laser confocal microscopy images of Cy5-miRNA-ICG-EVs showing uptake of EVs at different planes of UMSCC9 cells. Images were taken 10 h after incubation with Cy5-miRNA-ICG-EVs at a concentration of 12×10^9 . Each slice thickness is 1 μm , scale bar: 50 μm).

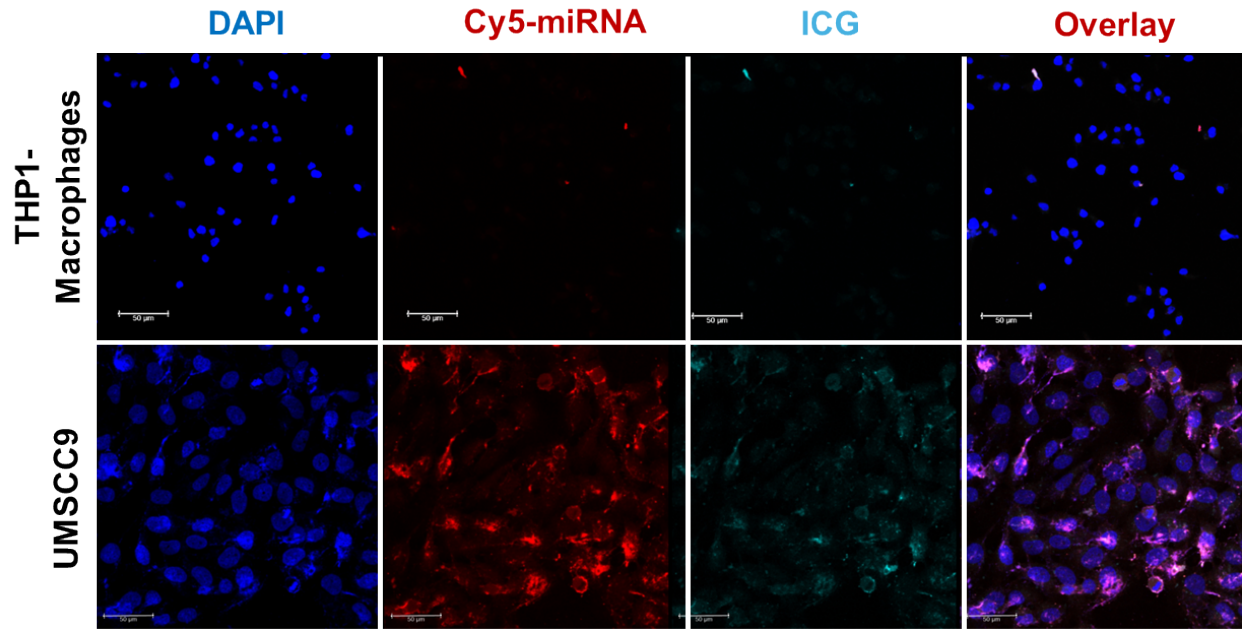


Figure S12. Cellular internalization analysis of Cy5-miRNA-ICG-EVs in THP1-macrophages and UMSCC9 cancer cells (Experimental conditions: 10 h incubation time; Concentration of Cy5-miRNA-ICG-EVs is 12×10^9 , scale bar: 50 μm).

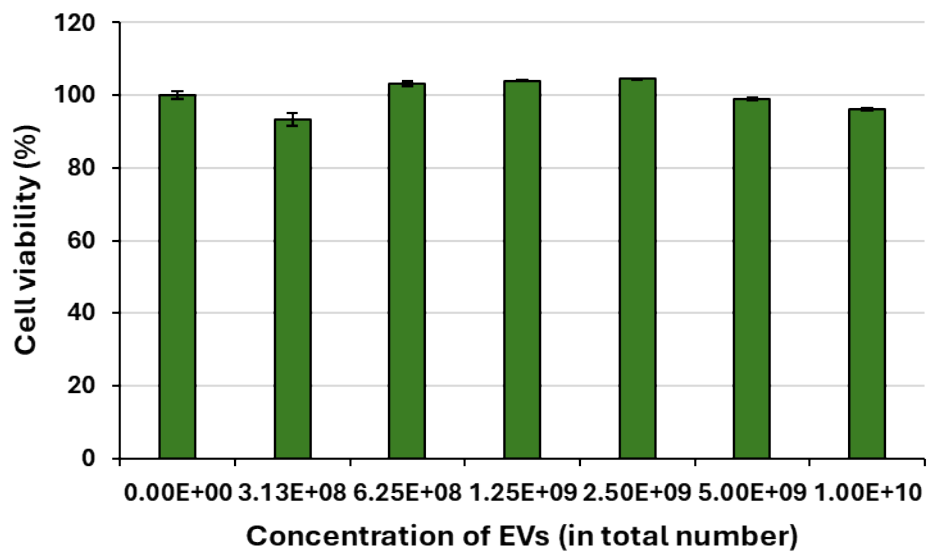
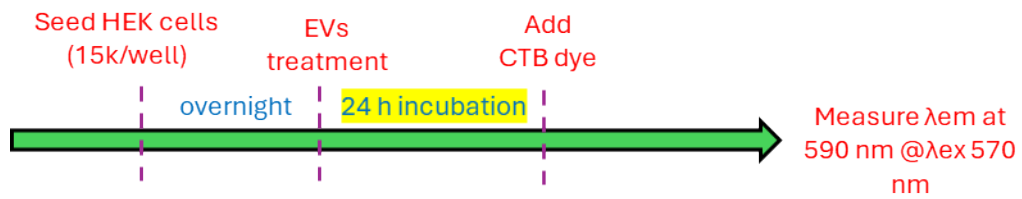


Figure S13. CTB assay measuring cell viability after treating HEK2923T cells with different concentrations of EVs for a period of 24 h.

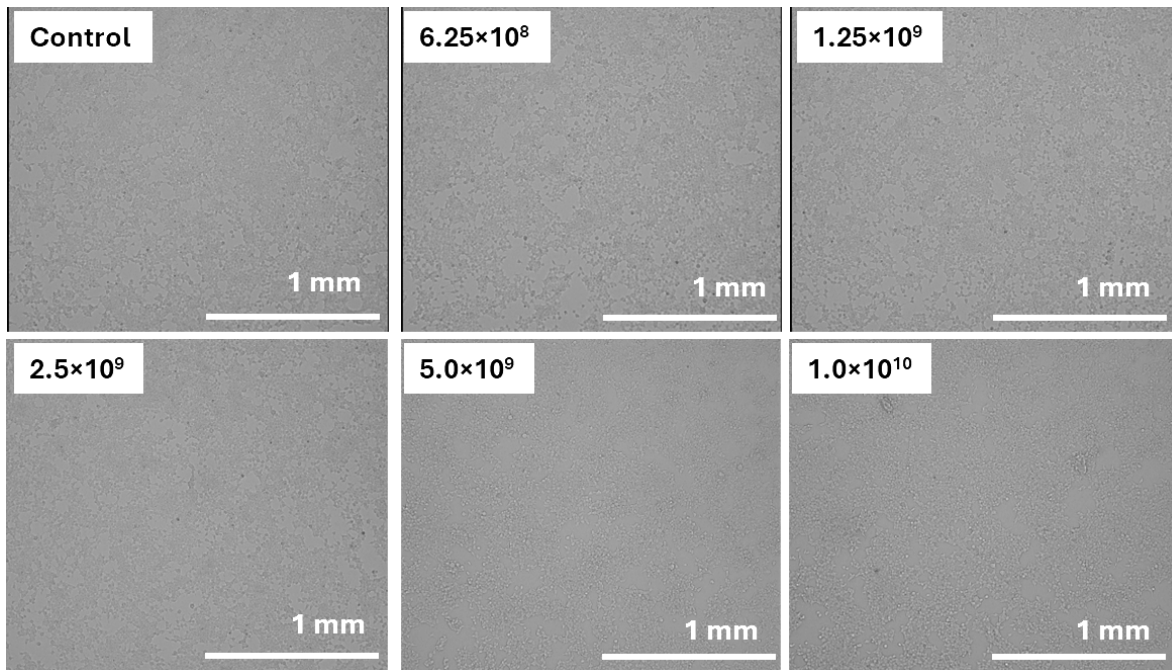


Figure S14. Celigo microscopy images measuring the HEK2923T cell growth (confluence) after treating with different concentrations of EVs for a period of 24 h.

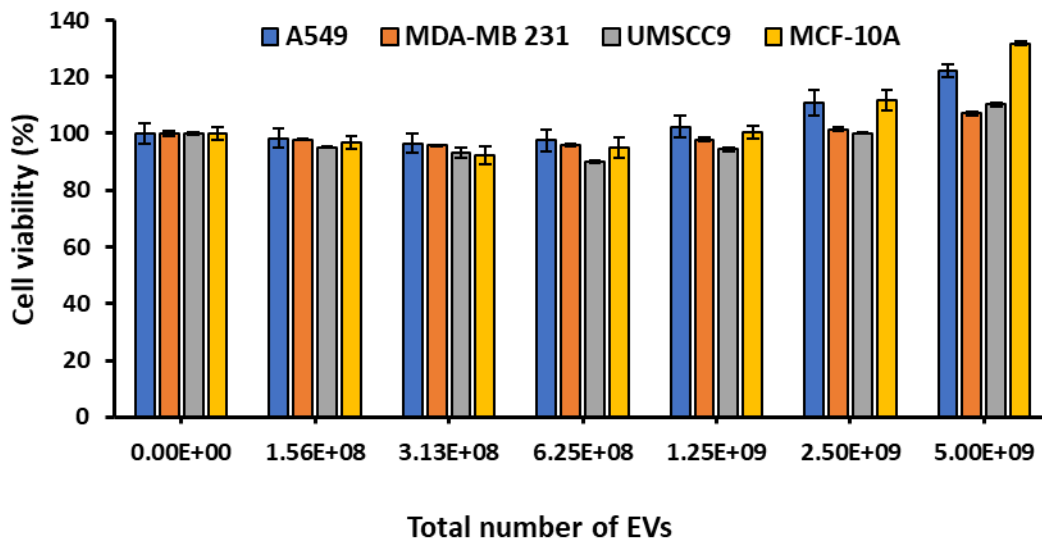


Figure S15. Cytotoxicity of UMSCC9 cell derived EVs evaluated in A549, MDA-MB-231 and UMSCC9 cancer cell lines, and MCF-10A normal cells. The assay was performed by incubating the cells with EVs for 24 h. Cell viability was evaluated using CTB assay.

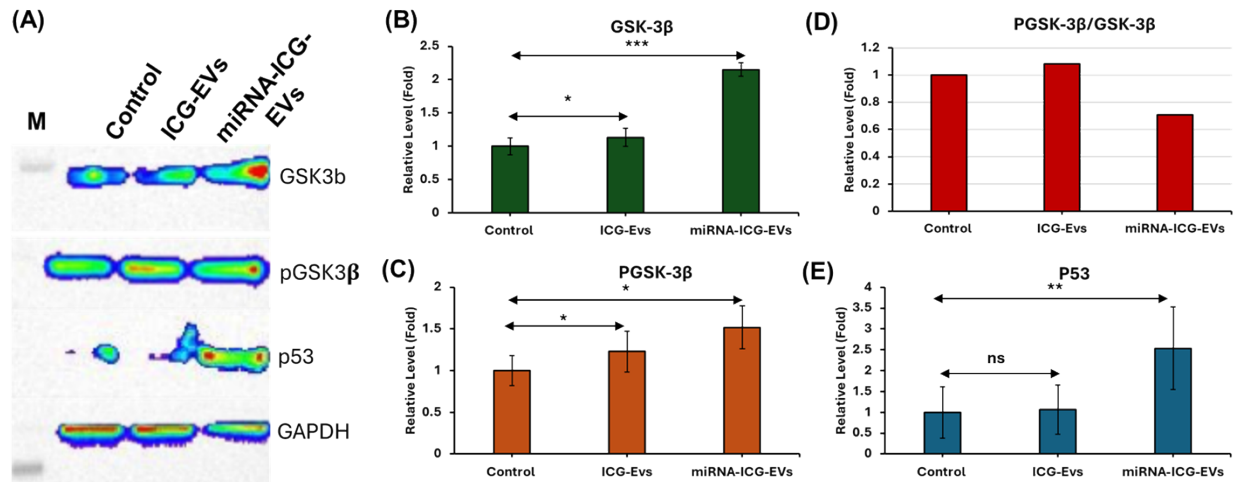


Figure S16. (A) Immunoblot analyses of protein isolated from UMSCC9 cells after treatment using ICG-EVs and miRNA-ICG-EVs in comparison to control cells for the expression of miR-10b target and its downstream mechanistic proteins. (B-E) Quantitative graph showing relative fold level of: GSK-3β (B); Phospho-GSK-3β (C); ratio between GSK-3β and pGSK-3β (D); and p53 (E). We used respective target specific primary antibody followed by anti-rabbit-IgG-HRP conjugate as secondary antibody for the detection. All the protein levels were normalized using GAPDH. P values corresponding to <0.05, <0.01, and <0.001 are denoted as *, **, and ***, respectively.

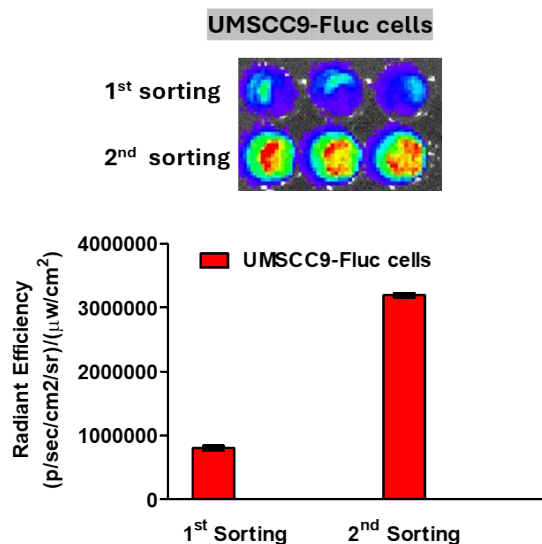


Figure S17. Bioluminescence images (top) and the quantitative plot showing the UMSCC9 cells engineered to stably express Firefly luciferase (FLuc) reporter gene.

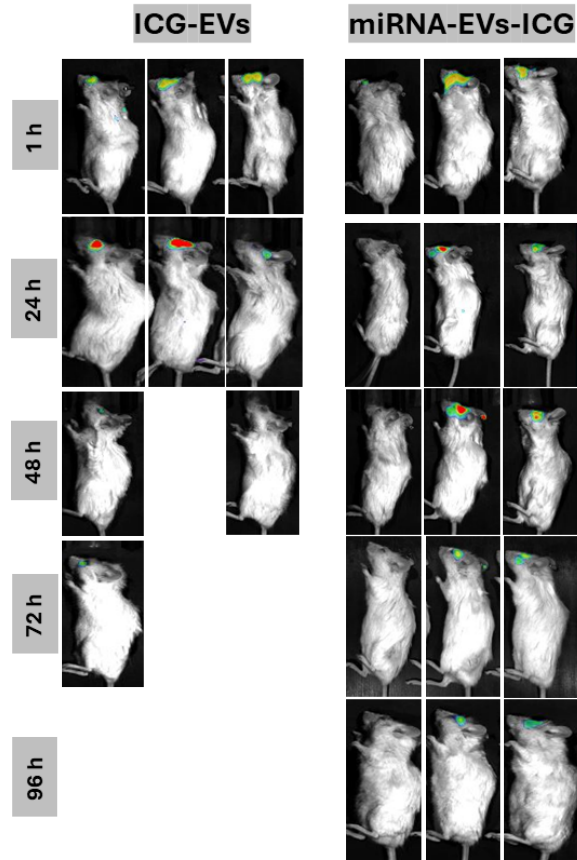


Figure S18. *In vivo* bioluminescence imaging of tumor bearing mice after administering the ICG-EVs and miRNA-ICG-EVs. (Note: Following 72 h of ICG-EVs administration to tumor-bearing mice, some of the mouse died in the ICG-EVs group likely owing to tumor burden while the mouse treated with miRNA-ICG-EVs remained alive under identical experimental conditions. As a result of the animal loss in the ICG-EVs group, we were unable to obtain imaging data at the 72- and 96-h time points and have therefore left those image panels blank.)

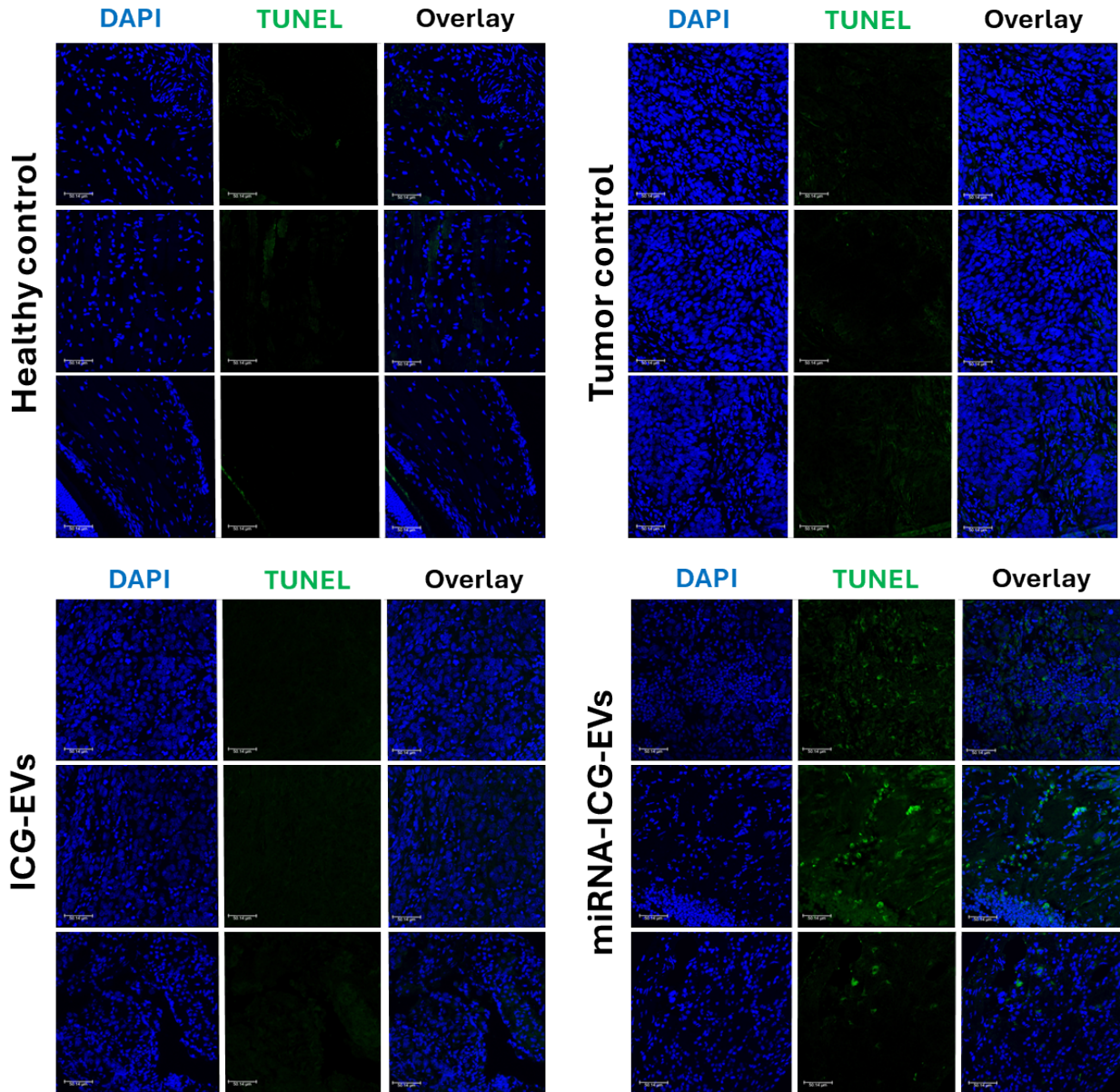


Figure S19. Additional fluorescence microscopic images of tissues from animals with different treatment groups such as healthy control (without tumor), tumor control (without treatment), ICG-EVs, and miRNA-ICG-EVs treated groups (Scale bars: 50 μ m).

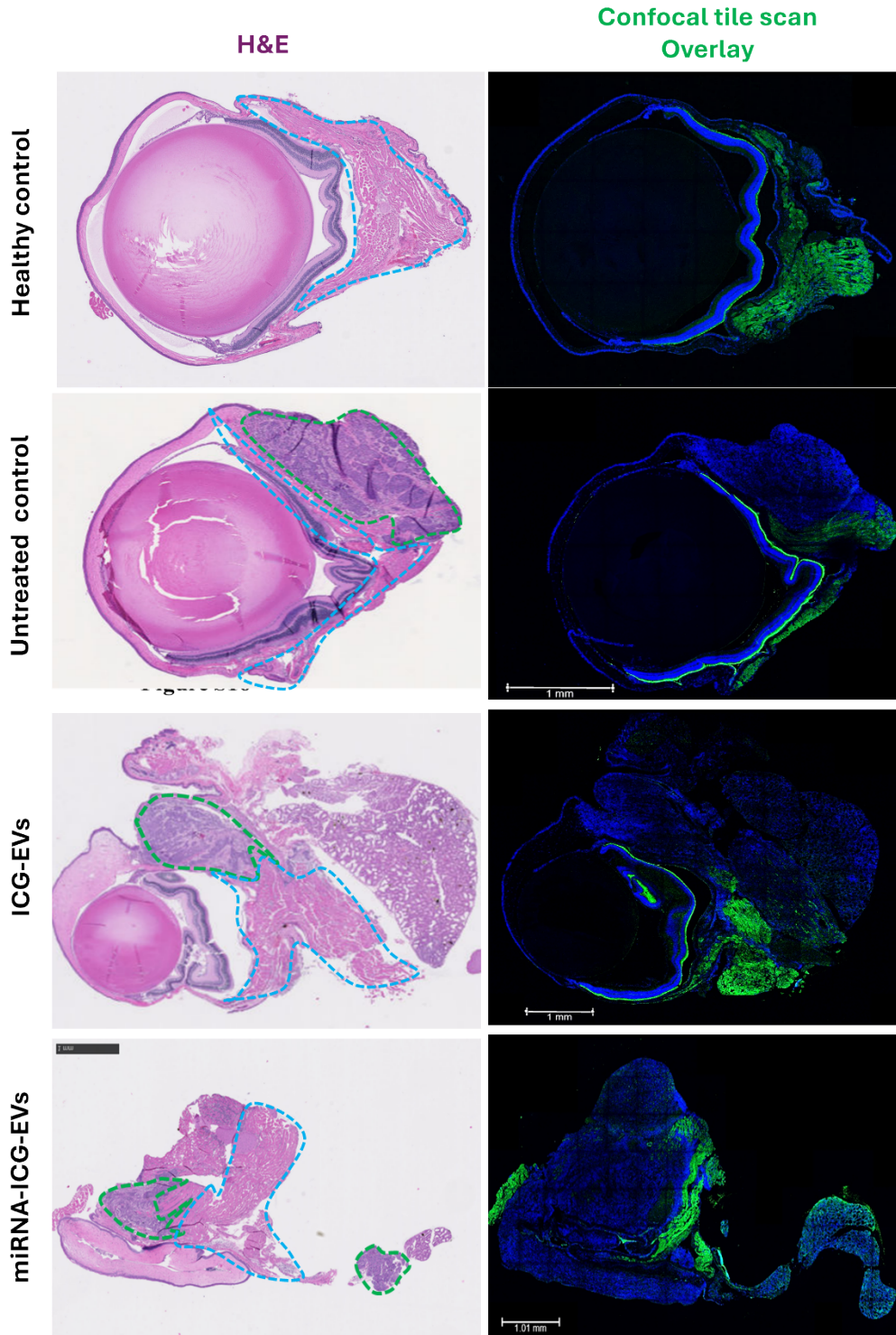


Figure S20. Digital H&E, and confocal fluorescent tile scan images of optic globe and surroundings showing the tumor from different groups, including healthy control, untreated control, and treatment groups with ICG-EVs and miRNA-ICG-EVs. Green dotted regions indicate the tumor area and blue dotted region indicates surrounding muscle (Scale bars: 1 mm).